Anisotropic Cascade of Field-Induced Phase Transitions in the Frustrated Spin-Ladder System BiCu_{2}PO_{6}

Yoshimitsu Kohama, Shuang Wang, Atsuko Uchida, Krunoslav Prsa, Sergei Zvyagin, Yuri Skourski, Ross D. McDonald, Luis Balicas, Henrik M. Ronnow, Christian Rüegg, and Marcelo Jaime

Phys. Rev. Lett. **109**, 167204 — Published 17 October 2012

DOI: 10.1103/PhysRevLett.109.167204

Anisotropic cascade of field-induced phase transitions in the frustrated spin-ladder system $BiCu_2PO_6$

Yoshimitsu Kohama,[1] Shuang Wang,[2,3] Atsuko Uchida,[1] Krunoslav Prsa,[2] Sergei Zvyagin,[4] Yuri Skourski,[4] Ross D. McDonald,[1] Luis Balicas,[5] Henrik M. Ronnow,[2] Christian Rüegg,[6,7,8] and Marcelo Jaime[1]

[1] MPA-CMMS, Los Alamos National Laboratory, Los Alamos, New Mexico 87545, USA

[2] Laboratory for Quantum Magnetism, Ecole Polytechnique Federale de Lausanne, CH-1015 Lausanne, Switzerland

[3] Laboratory for Developments and Methods, Paul Scherrer Institut, CH-5232 Villigen PSI, Switzerland

[4] Dresden High Magnetic Field Laboratory (HLD), Helmholtz-Zentrum Dresden-Rossendorf, 01328 Dresden, Germany

[5] National High Magnetic Field Laboratory, Tallahassee, Florida 32310, USA

[6] London Centre for Nanotechnology and Department of Physics and Astronomy, University College London, London WC1H 0AH, UK

[7] Laboratory for Neutron Scattering, Paul Scherrer Institut, CH-5232 Villigen PSI, Switzerland

[8] DPMC-MaNEP, University of Geneva, CH-1211 Geneva, Switzerland

$BiCu_2PO_6$ is a frustrated two-leg spin ladder compound with a spin gap that can be closed with a magnetic field of approximately 20T. This quantum phase transition and its related phase diagram as a function of magnetic field and temperature (*H*,*T*) are investigated up to 60 T by means of specific heat, magnetocaloric effect, magnetization, and magnetostriction measurements. In contrast to other gapped quantum magnets, $BiCu_2PO_6$ undergoes a series of unexpected first- and second-order phase transitions when an external magnetic field is applied along the crystallographic *c*-axis. The application of magnetic field along the *b*-axis induces two second-order phase transitions. We propose that the anisotropy and complex phase diagram result from the interplay between strong geometrical frustration and spin orbit interaction necessary for the description of this fascinating magnetic system.

Materials with a spin gap have recently attracted intense theoretical and experimental interest due to the occurrence of field-induced exotic ground states and unconventional (H,T) phase diagrams.[1-6] In $BiCu_2PO_6$ a spin energy gap between the singlet ground state and the first excited triplet states opens upon cooling, because of singlet correlations forming between pairs (dimers) of Cu^{2+} ions with S=1/2. This spin gap can be closed by applying a magnetic field $H = H_c$, hence inducing a quantum phase transition (QPT), resulting in the generation of a macroscopic number of triplet states (triplons) that occupy the Cu-dimers in the crystal lattice. The triplet excitations, because of interactions with next-nearest-neighbors and beyond, are dispersive and hence can propagate throughout the lattice. In the language of hard-core bosons,[7] the triplons have kinetic energy from their mobility in the lattice, and potential energy given by their interactions. Depending on the balance between the potential and the kinetic energy of the triplons, the field-induced ground states can be described as a Bose-Einstein condensate with uniform static order [1,2], as a Mott-insulating state with super-lattice order,[4] or even as a supersolid phase.[8] The kinetic energy of the triplons is strongly reduced by geometrical frustration, and frustration can lead to various exotic ground states.

The magnetic Cu^{2+} ions in the related quasi-2D system $SrCu_2(BO_3)_2$ are arranged in a Shastry-Sutherland frustrated lattice, and to date is the only material where a super-lattice structure of triplets has been investigated in depth.[3-4] An important step in this topical area of condensed matter physics is to find alternative systems to test theoretical approaches in different limits. In this letter, we report the first observation of a cascade of phase transitions through magnetization, specific heat and magnetostriction measurements as a function of magnetic field, resulting in an anisotropic (H,T) phase diagram for the frustrated two-leg ladder spin-gap system $BiCu_2PO_6$ under fields up to 60 T. The results are discussed in the context of potential magnetic field-induced superstructures of triplons and transitions between phases with different (commensurate/incommensurate) magnetic order.

$BiCu_2PO_6$ crystallizes in the orthorhombic *Pnma* structure and is composed of zigzag two-leg Cu ladders along the crystallographic *b*-axis.[9] Along the rung direction (*c*-axis), the CuO_4 plaquettes share corners and induce the rung coupling, J_{Rung}, mediated by Cu-O-Cu super-exchange interaction.[10] These rungs are stacked along the *b-axis* forming zigzag two-leg ladders and leading to geometrical frustration between the nearest-neighbor leg coupling J_{Leg}, and the next nearest-neighbor leg coupling J_{NNN}. Bi cations are positioned between each ladder, but spin interaction between ladders, J_{IL}, is possible due to Cu-O-O-Cu super-exchange paths.[10] The *bc* planes are separated by PO_4 tetrahedra, and interactions between the planes are believed to be very weak.[10,11]

The exchange interactions in $BiCu_2PO_6$ have recently been studied in detail by inelastic neutron scattering and magnetic susceptibility measurements on powder samples, and by numerical calculations, and are estimated to be J_{Leg} = 137.8K, J_{NNN} = 73.3K, and J_{Rung} = 58.4 K, respectively.[11] The potentially strong frustration between J_{Leg} and J_{NNN} suggests that the gapped spin-singlet ground state has an incommensurate dispersion.[11,12] NMR data were used to estimate the spin gap $\Delta_s/k_B \approx$ 38.3 K [13] which is consistent with the critical field $\mu_0 H_c \approx$ 22 T estimated from magnetization measurements in a polycrystalline sample.[10] J_{IL} cannot be accurately estimated because numerical simulations show it to be very sensitive to the choice of the other stronger exchange parameters.[10,11] This leads to some controversy regarding the field-induced ground state and the dimensionality of the spin system. Tomonaga-Luttinger liquid [10] and Ising ground states [12] have been predicted, but remain an open question in $BiCu_2PO_6$.

Single crystals of $BiCu_2PO_6$ were grown by the TSFZ technique in an image furnace (ModelFZ-T-10000-H-VI-VP, Crystal System. Inc., Japan) using four 300 W halogen lamps as heat sources, as described before.[9] Specific heat (C_p) and magnetocaloric effect (MCE) measurements were performed in a 35 T DC magnet. C_p *vs* T was obtained using both thermal relaxation time and dual slope techniques.[14] Specific heat capacity as a function of H was measured using an AC technique simultaneously collecting the MCE data.[15] The magnetic contribution to the specific heat, C_M, was obtained by subtracting the lattice contribution determined in its non-magnetic analog $BiZn_2PO_6$.[16] Longitudinal magnetostricion (MS) measurements were performed by using a fiber optic strain gauge in a 60 T pulsed magnet.[17] Magnetization measurements were performed in magnetic field up to 60T. [10] The magnetic moment of the sample was obtained by integration of the voltage induced in a compensated pick-up coil system surrounding the sample. Details of the experimental procedure are described elsewhere.[10] The field dependence of the magnetization $M(H)$ was calibrated with low field magnetization data measured through nuclear magnetic resonance (NMR) (see, for instance, Kodama et al. [18] for a detailed discussion of how NMR data can be used to quantify magnetic moments in frustrated magnets), and a Quantum Design® Vibrating Sample Magnetometer.

Magnetization data for three different magnetic field orientations, *i.e.* parallel to the main crystallographic axes, are shown in Fig.1. Depending on the field orientation, the magnetization data show a finite slope at low magnetic fields. Upturns corresponding to the closure of the spin gap are observed at $\mu_0 H_c$ = 23, 21, and 20 T for magnetic fields applied along the *a*-, *b*-, and *c*-axis, respectively, in good agreement with $\mu_0 H_c \approx$ 22 T measured on a polycrystalline sample.[10] For $H//a$, a smooth magnetization curve is observed above H_c within the noise level of our measurement. On the other hand, for fields applied along the *b*- and the *c*-axis, the $M(H)$ curves show unexpected transitions at $\mu_0 H \approx$36 T, ≈34 T and ≈40 T, respectively.

The relative crystal length changes in the *a*-, *b*-, and *c*-axes ($\Delta L/L$) are shown in Figs.2(a), (b), and (c), respectively. When magnetic field is applied parallel to the *c*-axis, $\Delta L/L$

shows a sharp increase at H_c and two additional steps at higher fields. These steps persist up to 5.7 K and are similar to the $M(H)$ curves at the corresponding temperatures (Inset of Fig.1). Below 6 K, MS measurements detect that both high field anomalies display strong hysteresis as a function of field, suggesting first-order phase-transitions. Accordingly, MCE measurements in DC fields detect an irreversible heat release on both field up- and down-sweep as shown by the orange curve in Fig.4 (a). The observed heating reveals the presence of dissipation and/or irreversibility which can be the signature for first-order phase transitions.[15,19] Taken together, hysteresis in $\Delta L/L$ and irreversible heating in MCE, provide firm evidence that the anomalies correspond to first-order phase-transitions. When magnetic field is applied along the *a*- and the *b*-axis, the $\Delta L/L$ curves exhibit broad structures. For $H//b$, two broad anomalies can be seen at H_c and at $\mu_0H \approx 35$ T. The broad anomaly at higher field (indicated by an arrow) seems to be connected to the observed magnetization steps. Accordingly, it appears where the MCE data show heating and cooling as seen in Fig.4 (b). Symmetric MCE curves are typically seen at second-order phase boundaries.

Figs.3 (a) and (b), show the magnetic contribution to the specific heat, $C_M(T)$ for $H//b$ and $H//c$ respectively. Above H_c, $C_M(T)$ exhibits λ-type anomalies for both $H//c$ and $H//b$. Sharp anomalies are characteristic of long-range magnetic ordering, rather than a crossover expected for low dimensional systems.[6] When a magnetic field is applied along the *b*-axis, the peak position in temperature and the size of the anomaly monotonically grow with increasing field. On the other hand, for $H//c$ the peak position in temperature first increases, and then splits into two peaks above 33 T. Figure 3(c) and (d) show the magnetic-field dependence of C_M, for $H//c$ and $H//b$, respectively. In the spin-gapped region, $H<H_c$, $C_M(H)$ monotonically increases as the magnetic field increases. This tendency is attributed to the increase of triplet excitations, which are activated as the spin gap is closed. At $H = H_c$ a sharp peak emerges, which shifts to higher fields as the temperature increases. The position of the peak at different temperatures is used to construct the (H,T) phase diagram, yielding a very good agreement among the $C_M(T)$, magnetization, MS and MCE results. When the external magnetic field is applied parallel to the *c*-axis, $C_M(H)$ suddenly drops above $\mu_0H = 32$ T. Below 2K, a broad anomaly develops around $\mu_0H \approx 30$ T. The complex shape of $C_M(H)$ reflects the occurrence of a series of field-induced phase transitions. For $H//b$, a tiny kink was observed below 1.3 K (indicated by arrow). The kink originates from a second-order phase transition, as indicated by symmetric MCE curves.

Figure 4 summarizes the phase boundaries in $BiCu_2PO_6$ for fields applied parallel to the *b*- and *c*-axis, constructed from the C_p, MCE, and MS measurements. Open symbols indicate what are likely to be first-order phase boundaries, whereas solid symbols indicate possible second-order phase boundaries. The anisotropy above the QPT at H_c implies that the observed ordered states (II, III, IV, or V) likely have different spin structures.

Field-induced QPTs in gapped quantum spin systems have been studied in a number of compounds, of which the highly frustrated Shastry-Sutherland system $SrCu_2(BO_3)_2$ is a remarkable example. In this material the transitions at high magnetic fields are accompanied by magnetization steps, evidence of magnetic texture originated in strong geometric frustration. In this letter we show for the first time that $BiCu_2PO_6$, whose backbone is formed by coupled, frustrated spin ladders, also exhibits a series of second and first-order phase transitions above a field-induced QPT. Additionally, as shown in Fig.1, we observe strongly anisotropic critical fields and a linear magnetization vs field in the spin gapped region. These indicate that $BiCu_2PO_6$ has a strong spin-orbital interaction which leads to Dzyaloshinksy-Moriya term and *g*-factor anisotropy. Spin-orbital interaction, intrinsically anisotropic, produces off-diagonal Dzyaloshinski-Moriya terms that allow spin-level mixing and a linear M(H) dependence for $H < H_c$.[10] The combined effects of strong magnetic frustration and spin-orbital interaction could also account for the anisotropy, and complexity of the phase diagram displayed by BiCu2PO6.

Indeed, geometrical frustration is likely to favor the localization and lead to the formation of magnetic texture and concomitant magnetization plateaus in $BiCu_2PO_6$. The observed upturns in $M(H)$ (Fig. 1), however, are followed by concave shoulder-like regions between features rather than plateaus expected for an incompressible magnetic state. This important characteristic of the data could be a hint for the formation of a spin super-solid as proposed by Sengupta *et al*.[8] However, in addition to the lack of estimation of J_{IL}, the geometrical frustration renders it difficult to apply simple quantum Monte Carlo approaches to $BiCu_2PO_6$. An alternative scenario may be novel transitions between phases with different commensurate/incommensurate spin structures, similar to those reported in the frustrated quasi-1D quantum spin chain materials Cs_2CuCl_4 [20,21] and $BaCu_2Ge_2O_7$[22]. In these systems, the observed anisotropic phase diagrams are likely due to spin-orbital interaction. The magnetization magnitude at the fields where steps occur may be also consistent with this picture. However, it should be pointed out that there is no spin gap in Cs_2CuCl_4 and $BaCu_2Ge_2O_7$. A field-induced anisotropic commensurate-incommensurate transition has not been found in any other spin-gapped ladder systems. The high magnetic fields at which these features are observed make additional experimental studies such as by elastic/inelastic neutron scattering quite difficult.

In conclusion, we present the (H,T) phase diagram of $BiCu_2PO_6$, a new frustrated gapped quantum magnet, up to 45 T. Anisotropic transitions are observed at high magnetic fields, that have not been reported for other low dimensional spin gap systems. The anisotropic and remarkably complex phase boundaries possibly arise from the interplay between spin-orbital interaction and geometric frustration. More theoretical work is needed to be able to fully understand field-induced phase transitions in such frustrated quasi-1D ladder systems. On the experimental side, high-field NMR could be important to elucidate the spin structure of the different regions of the phase diagram.

Acknowledgements

We thank A. Feiguin and F. Casola for fruitful discussions, Li Gang and E. D. Mun for assistance during experiments, and S. A. Crooker for his contributions and assistance with the optical FBG Magnetostriction measurement. Y.K., A.U., R.D.M., and M.J. were supported by US-DOE, NSF through NSF-DMR-0084173 and the State of Florida. Y.K. was also partially supported by The Institute for Solid State Physics. L. B. is supported by DOE-BES through award DE-SC0002613. This work was partially supported by the DFG and EuroMagNET II (EU contract No. 228043). Work in Switzerland was supported by the Swiss NSF under MaNEP and Division II.

[1] S. E. Sebastian, et al., *Nature* **441**, 617-620 (2006).

[2] V. S. Zapf, et al., *Phys. Rev. Lett*., **96**, 077204 (2006).

[3] Ch. Rüegg, et al., *Nature* **423** 62-65 (2003).

[4] S. E. Sebastian, et al., *Proc. Natl. Acad. Sci*., **105**, 20157-20160 (2008)

[5] M. Jaime, *et al*., *Proc. Natl. Acad. Sci.,* **109**, 12404-12407 (2012).

[6] Ch. Rüegg, et al., *Phys. Rev. Lett*., **101**, 247202 (2008).

[7] T. Giamarchi, *et al*., *Nature Physics* **4**, 198-204 (2008).

[8] P. Sengupta and C.D. Batista, Phys. Rev. Lett. **98**, 227201 (2007). *Idem*, Phys. Rev. Lett. **99**, 217205 (2007).

[9] S. Wang, et al., *J. Crystal Growth* **313**, 51-55 (2010).

[10] A. A. Tsirlin, *et al.*, *Phys. Rev. B* **82**, 144426 (2010).

[11] O. Mentré, et al., *Phys. Rev. B* **80**, 180413(R) (2009).

[12] A. Lavarelo, G. Roux, and N. Laflorencie, *Phys. Rev. B* **84**, 144407 (2011).

[13] F. Casola, et al., *Phys. Rev. Lett*. **105**, 067203 (2010).

[14] S. Riegel and G. Weber, *J. Phys. E: Sci. Instrum*., **19** 790 (1986).

[15] Y. Kohama, C. Marcenat, T. Klein, and M. Jaime, *Rev. Sci. Instrum.* **81**, 104902 (2010).

[16] B. Koteswararao, A. V. Mahajan, L. K. Alexander, and J. Bobroff, J. Phys.: *Condens. Matter* **22**, 035601 (2010).

[17] R. Daou, et al., *Rev. Sci. Instrum.* **81**, 033909 (2010).

[18] K. Kodama, et al., *Science* **298**, 395 (2002).

[19] A.V.Silhanek, et al., *Phys. Rev. Lett*. **96**, 136403 (2006).

[20] R. Coldea, et al., *Phys.Rev. Lett.* **79**, 151-154 (1997).

[21] O. A. Starykh, H. Katsura, and L. Balents, *Phys. Rev. B* **82**, 014421 (2010).

[22] A. Zheludev et al., *Phys.Rev. Lett.* **78**, 4857 (1997).

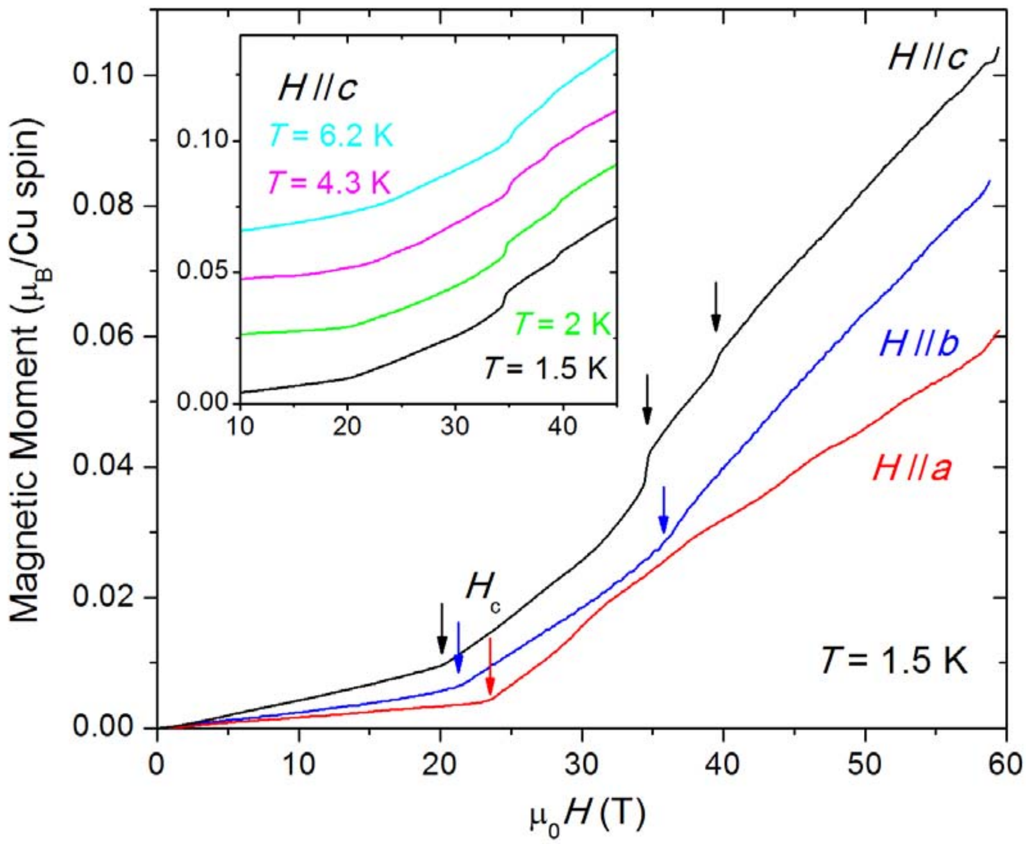

Fig.1. (color online). Magnetization M vs H for *H//a* (red), *H//b* (blue), and *H//c* (black). Inset: M vs H for *H//c* measured at different temperatures (the experimental data are vertically displaced for clarity).

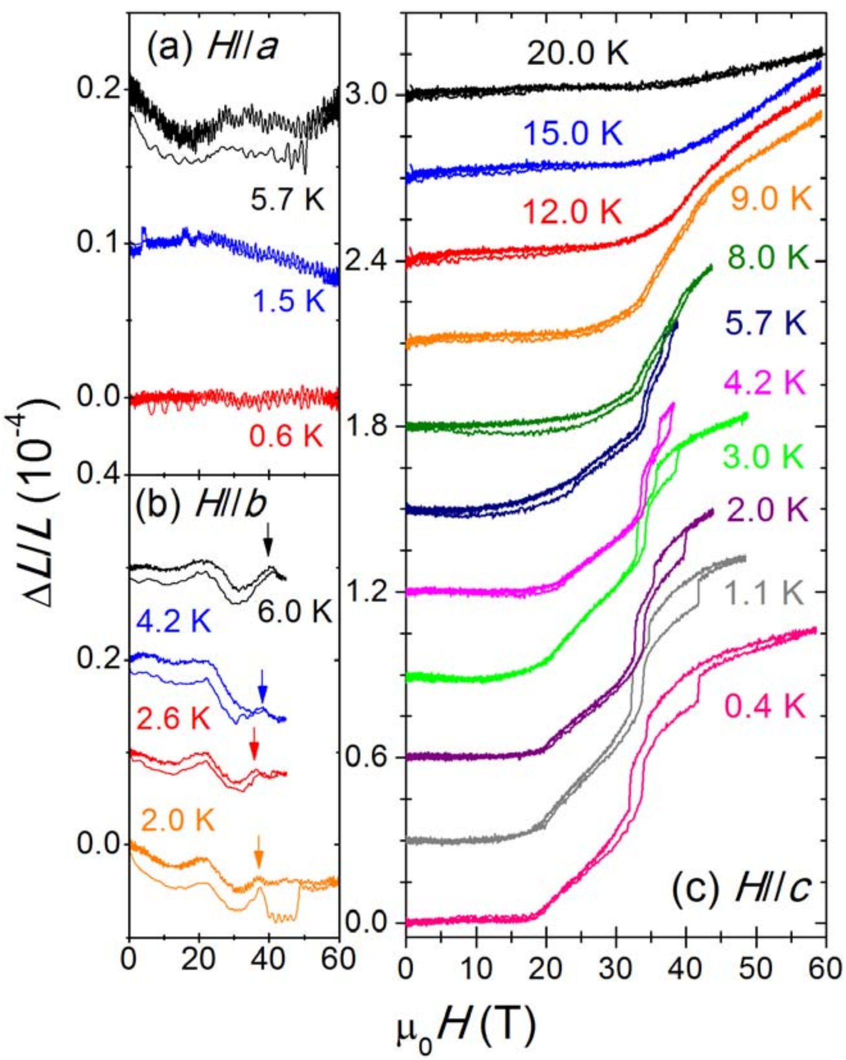

Fig.2 (color online). Magnetostriction $\Delta L/L$ vs H, for $H//a$ (a), $H//b$ (b), and $H//c$ (c). For clarity, the data at different temperatures were shifted vertically.

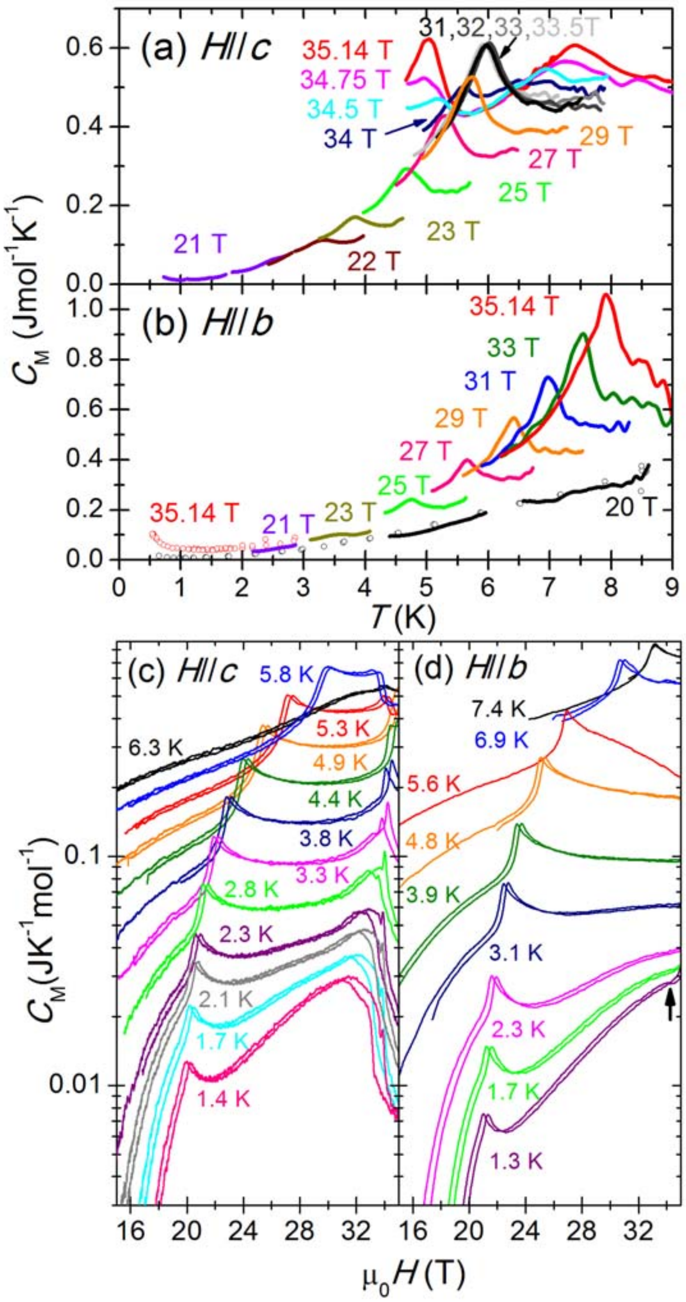

Fig.3 (color online). Specific heat C_M vs T for $H//c$ (a) and $H//b$ (b). The low temperature upturn in C_M is due to a nuclear Schottky anomaly. C_M vs H for $H//c$ (c) and $H//b$ (d). The temperature stability was 3% during magnetic field sweeps.

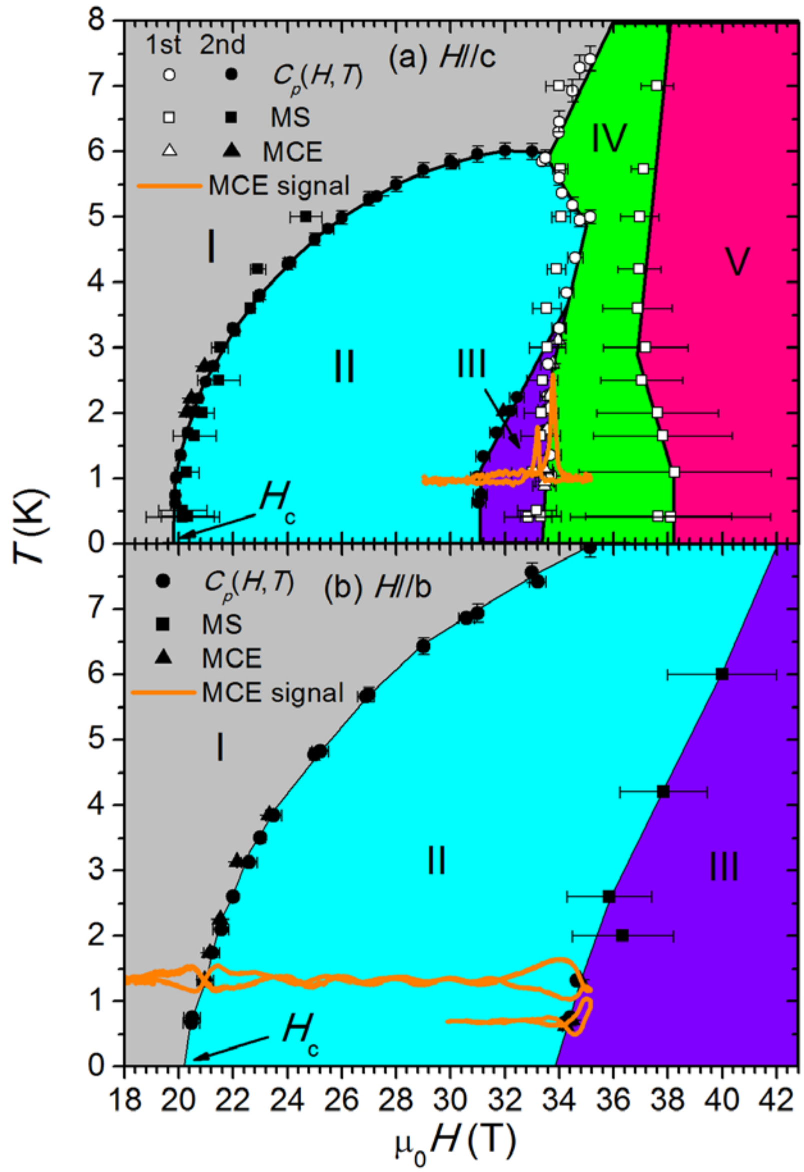

Fig.4. (color online). Magnetic phase diagram for (a) *H//c* and (b) *H//b* deduced from the C_p (circles), MS (squares), and MCE (triangles) measurements taken at various temperature and as a function of magnetic field. The error bars are evaluated from the size of the hysteresis and the width of the peaks. The orange curves correspond to MCE data measured in a 35T DC magnet. (a) The MCE traces have been multiplied by a factor of 10. (b) MCE traces for H//b have been multiplied by 100 (at 1.3 K) and 50 (at 0.7 K), respectively.